ELSEVIER

International Journal of Solids and Structures 41 (2004) 1565–1580

INTERNATIONAL JOURNAL OF SOLIDS and STRUCTURES

www.elsevier.com/locate/ijsolstr

Transition from progressive buckling to global bending of circular shells under axial impact—Part I: Experimental and numerical observations

D. Karagiozova [a,*,1], Marcílio Alves [b,*]

[a] *Institute of Mechanics, Bulgarian Academy of Sciences, Acad. G. Bonchev St., Block 4, Sofia 1113, Bulgaria*

[b] *Department of Mechatronics and Mechanical Systems Engineering, University of São Paulo, São Paulo, SP 05508-900, Brazil*

Received 11 February 2003; received in revised form 1 October 2003

Abstract

The influence of impact velocity and material characteristics on the dynamic buckling response of circular shells subjected to axial impact loads is studied. It is shown experimentally that the critical buckling length, which marks the transition between progressive and global buckling of aluminium alloy circular tubes, is significantly influenced by the axial impact velocity. A finite element analysis is undertaken to further explore the effects of material yield stress, strain hardening and strain rate sensitivity on the transition phenomenon. It is observed that circular tubes made of ductile alloys with a high yield stress and low strain hardening characteristics have a better performance as energy absorbers than tubes made of alloys with a low yield stress and high strain hardening characteristics. Theoretical analysis of some particular features of the dynamic buckling transition is presented in Part II [International Journal of Solids and Structures (2004)].

Keywords: Progressive buckling; Global bending; Axial impact; Energy absorption; Buckling transition

1. Introduction

An efficient design of energy absorption devices can be achieved using thin-walled tube-like structures, which have been extensively studied and comprehensive reviews can be found in (Alghamdi, 2001; Jones, 1989a; Johnson and Reid, 1978; Reid et al., 1993; Reid, 1993). The majority of studies on energy absorbing devices are usually concerned with the influence of the geometry of the device on its efficiency and various recommendations are given on that matter. Recently, shell-like structures filled in with foams are shown to have very good energy absorbing properties when subjected to a quasi-static (Chen and Wierzbicki, 2001) or dynamic axial load (Hanssen et al., 2002).

* Corresponding authors.

E-mail addresses: d.karagiozova@imbm.bas.bg (D. Karagiozova), maralves@usp.br (M. Alves).

[1] Tel.: +55-11-30915757; fax: +55-11-30915461.

0020-7683/$ - see front matter © 2003 Elsevier Ltd. All rights reserved.
doi:10.1016/j.ijsolstr.2003.10.005

Nomenclature

A	cross-section area of a shell
E, E_h	the Young's modulus and hardening modulus, respectively
F	axial force at the proximal end of a shell
G	impact mass
L	length of a shell
L_{cr}^{static}	static critical length for the transition between progressive buckling and global bending
L_{cr}^{dyn}	dynamic critical length for the transition between progressive buckling and global bending
R	radius of a shell
T_b	bending energy
T_c	compression energy
T_0, T_k	initial and current kinetic energies, respectively
T_p	plastic energy dissipation
V_0	initial impact velocity
h	thickness of a shell
t	time
t^*	time at the end of the compression phase
u	axial displacement at the proximal end of a shell
σ_0, σ_e	material flow stress and equivalent stress, respectively
g	subscript for global buckling, Fig. 15
p	subscript for progressive buckling, Fig. 15

The optimisation of energy absorbing devices usually assumes that a particular geometry will promote a progressive buckling mechanism (Alexander, 1969; Jones, 1989b), which is maintained throughout the response. It is also anticipated that the introduction of a mechanical denting (trigger) is sufficient to control the appearance of the first wrinkle when a shell-like structure is loaded quasi-statically. Dynamic loads, however, influence not only the material properties due to strain-rate sensitivity effects but also affect the buckling pattern (Karagiozova et al., 2000; Karagiozova and Jones, 2000–2002) due to inertia effects. Moreover, the actual stress–strain relationship in the plastic range can influence the buckling pattern in sufficiently long circular shells (Karagiozova and Jones, 2002). In this case, an introduction of a trigger is not necessarily sufficient to initiate a desirable buckling mode.

The initiation of the desired buckling mode becomes even more complicated when long shell-like structures are to be used to absorb the impact energy as these structures can exhibit additional buckling modes leading to poor energy absorption. In particular, buckling modes similar to the Euler buckling mode characteristic for statically loaded rods or higher dynamic 'rod' modes can develop in long tubes (global bending) as shown experimentally by Andrews et al. (1983) and Abramowicz and Jones (1997) depending on the geometry, boundary conditions and material of the structure.

The threshold conditions between quasi-static progressive buckling and global bending of circular tubes depend on the ratios $2R/h$ and $L/2R$, as first reported by Andrews et al. (1983) for aluminium tubes and recently by Guillow et al. (2001) for aluminium alloy tubes. It is shown experimentally that a static critical tube length, L_{cr}^{static}, exists for a particular ratio, $2R/h$, so that tubes shorter than this length collapse progressively while longer tubes develop a global bending mode.

Similar observations were reported by Abramowicz and Jones (1997) where they considered the response of long circular and square mild steel tubes. The authors report also experimental results from tests of

dynamically loaded circular and square shells subjected to axial impacts with initial velocities between 5 and 12 m/s, approximately, which show that the critical length for the buckling transition increases when the tubes are loaded dynamically. This observation was attributed to the increased lateral inertia of the shell.

The importance of inertia effects on the buckling phenomenon of various axially loaded structures is also discussed in other references (Karagiozova and Jones, 1996; Karagiozova et al., 2000; Karagiozova and Jones, 2000; Su et al., 1995), so that it is reasonable to postulate that tubes with a particular cross-section may exhibit global or progressive collapse when varying the impact velocity. Hence, the transition conditions from global to progressive collapse could be sought as a function of the initial velocity of the axial impact load, V_0. Thus, an ideal mechanism for impact energy absorption using tubes, called dynamic progressive buckling (Jones, 1989b), can occur in axially loaded shells provided some conditions related to the tube's material and geometry, boundary and initial conditions are met.

Due to the complexity of the dynamic buckling transition, the existing analytical models aimed at establishing a criterion for the boundary between progressive and global buckling reported by Abramowicz and Jones (1997) and Mahmood and Paluszny (1982) consider only the quasi-static response. Lu and Mao (2001) assume small strains and a quasi-static approach, to investigate the influence of the shell geometry on triggering a particular buckling mode shape, focusing on the critical loads and mode shapes. Recently, a numerical study of the dynamic buckling transition of aluminium alloy square tubes was reported by Jensen et al. (2002), where it was noted that the critical length for the buckling transition varied depending on the width-to-thickness ratio and impact velocity.

A systematic investigation has been pursued by the authors aimed at understanding further the phenomenon of dynamic transition response of cylindrical shells with special emphasis on the influence of the impact velocity and preliminary results are reported in references (Alves and Karagiozova, 2001, 2002). These studies evolved to the present two-part article, which explores the influence of the axial impact velocity on the buckling modes of circular cylindrical shells.

In this Part I paper, Section 2 describes the experimental set-up and results, which provide a basis for the finite element analysis presented in Section 3. Section 4 discusses in detail various features of the buckling transition phenomenon as revealed by the experimental and numerical results. In the sequel Part II paper (Karagiozova and Alves, 2004), mathematical models are developed in order to give some further insight into the influence of the various parameters on the complex phenomenon of buckling transition.

2. Experimental observations

Aluminium alloy tubes of external diameter 50.8 mm and thickness 2 mm were loaded axially both quasi-statically (by using a compression testing machine) and dynamically (by using a drop mass test rig). In order to obtain the material data, a quasi-static material test was performed on a strip cut from a shell using a standard tensile test machine and the resulting stress–strain relationship is shown in Fig. 1. The elastic modulus of this material is 70 GPa and the density is $\rho = 2700$ kg/m^3. It is assumed that the mechanical properties of this aluminium alloy are not sensitive to strain rate at room temperature.

The tubes, freely supported at both ends, were initially tested in a compression testing machine. By varying the tube length, it was possible to find a length threshold capable of triggering a global or progressive mode of collapse as indicated in Fig. 2. A critical quasi-static length of $L_{\mathrm{cr}}^{\mathrm{static}} = 315$ mm was found. It was observed that a variation of just 1 mm around this critical length was capable of triggering either a progressive or a global mode of collapse.

Impact loads were applied to the tubes using a drop hammer with a mass $G = 120$ kg released from different heights. The drop height was controlled by a computer with an accuracy of ±5 mm. The dynamically tested tubes were 360, 500 and 650 mm long and rested freely on a platform during the initial

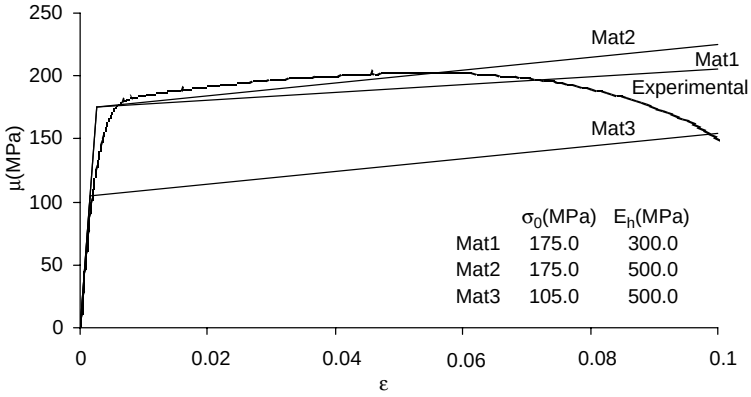

Fig. 1. True stress–true strain characteristic of the aluminium alloy (Experimental). *Mat*1 and *Mat*2 represent two bilinear models used in the simulations; *Mat*3 is used as a material model with a low yield stress.

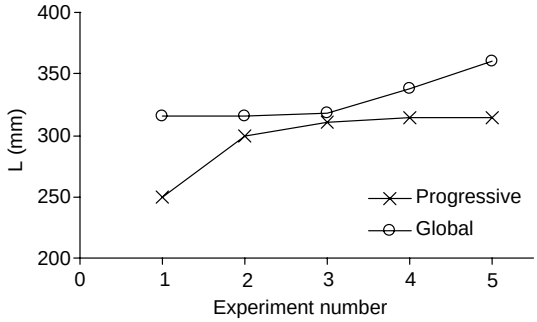

Fig. 2. Quasi-static buckling transition length for the aluminium alloy tubes.

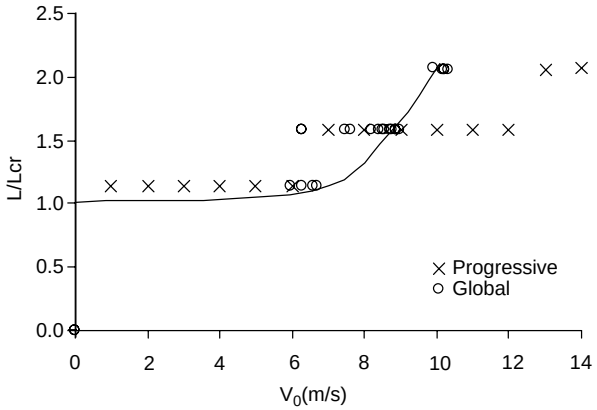

Fig. 3. Influence of the impact velocity on the dynamic buckling transition of aluminium alloy tubes.

contact between the tube and striker. The platform has a mass of 3700 kg, so that it can be assumed that no energy loss occurs during the impact event.

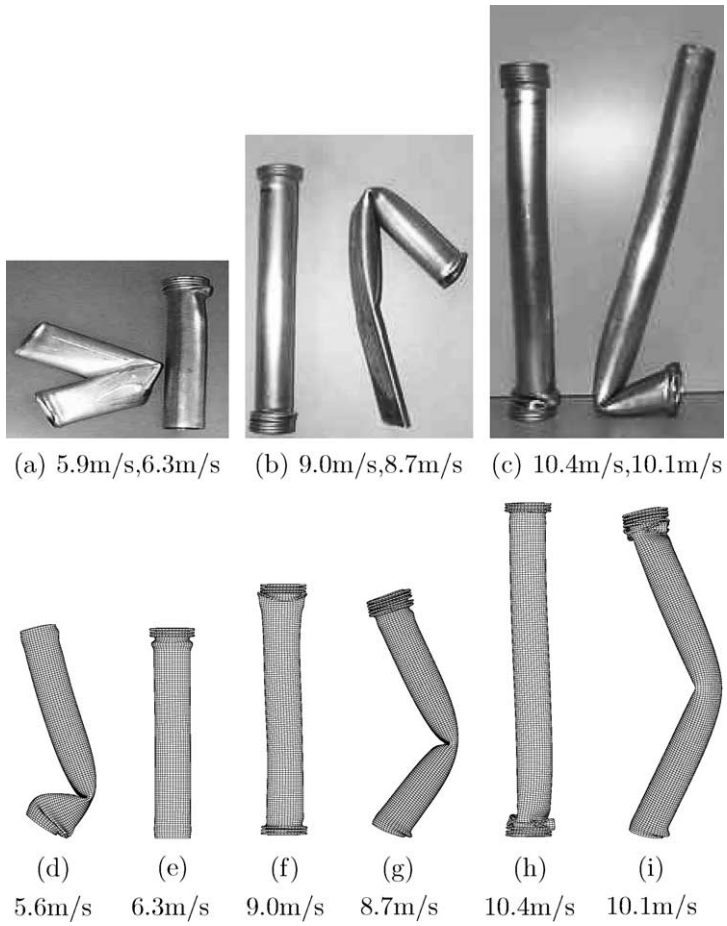

Fig. 4. Experimental (top row) and numerical simulation of tubes (bottom row) with (a,d,e) $L = 360$ mm, (b,f,g) $L = 500$ mm and (c,h,i) $L = 650$ mm subjected to a 120 kg impact mass. The labels indicate the impact velocity.

This set-up allowed the authors to explore the influence of impact velocity on the dynamic critical length at the transition from dynamic progressive buckling to global bending collapse. A summary of the experimental results is shown in Fig. 3, where it is evident that the impact velocity plays an important role in regard to the transition between the two collapse modes. The higher the impact speed, the more stable the tube, i.e. progressive buckling can occur for longer tubes. Fig. 3 indicates the dynamic critical length, L_{cr}^{dyn}, has increased more than twice L_{cr}^{static}. Fig. 4 (top row) shows progressive and global modes of collapse for tubes having $L = 360$ mm, 500 mm and 650 mm at the corresponding critical impact velocities.

3. Numerical model and verification

Numerical simulations of an axial impact on long tubes having the same cross-sectional characteristics as the ones tested was carried out using the FE code ABAQUS/Explicit. Shell elements RS4 (3.9 mm × 3 mm) were used to model all the analysed tubes. The load is applied as a point mass attached to the nodes of a rigid body which had an initial velocity, V_0. The contact between the shell and striker and between the distal

end of the shell and rigid surface was defined using the 'surface interaction' concept together with a friction coefficient of 0.25 at both ends. Any self-contacts of the inner and the outer surfaces of the shell were assumed frictionless.

In order to trigger asymmetric buckling patterns, initial imperfections corresponding to the first two elastic buckling modes of a shell were introduced. The first buckling mode for a 500 mm long shell is shown in Fig. 5. The second buckling mode has the same shape as the first one but is perpendicular to the plane shown in Fig. 5. The magnitude of the maximum amplitude of these modes was selected in a way to reproduce the experimental threshold velocity in Fig. 3 for a tube with $L = 500$ mm. It turned out that a maximum magnitude of 0.0005 L for these two buckling modes gives an adequate representation of the corresponding experimental results in terms of the final buckling shapes and crushing distances (in the case of progressive buckling) for all three tube lengths tested.

This strategy of introducing initial geometrical imperfections corresponding to the first two elastic buckling modes of a shell with magnitudes 0.0005 L was used throughout the numerical simulations in the present study and good agreement between the test responses of the 360 mm, 500 mm and 650 mm long tubes and the corresponding numerically predicted final buckling shapes is evident in Fig. 4 and Table 1. The selected magnitude of the initial imperfections is consistent with the standard requirements for aluminium extrusions (Mazzolani, 1985) prescribing maximum deviation of 0.001 L with respect to the longitudinal axis of a circular tube.

Some recent studies of the dynamic buckling of circular tubes (Karagiozova et al., 2000; Karagiozova and Jones, 2001, 2002) show that not only the impact velocity but the material properties as well play an important role in this complex phenomenon. An interpretation of the buckling transition using a non-linear stress–strain relationship leads to a very complex analysis due to the initial compression of a shell, which is associated with different hardening slopes depending on the loading parameters. Therefore, three different bilinear material models (Fig. 1) were used in the numerical simulation in order to explore the influence of

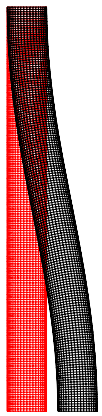

Fig. 5. First elastic buckling mode for a tube with $L = 500$ mm.

Table 1
Deformation length at transition velocities (progressive buckling)

L (mm)	360	500	650
V_0 (m/s)	6.3	9.0	10.4
δ_{exp} (mm)	62.7	146.1	191.4
$\delta_{numeric}$ (mm)	63.0	154.3	190.5

the material parameters on the buckling transition, namely the flow stress and strain hardening. Materials *Mat*1 and *Mat*2 have the same yield stress of 175 MPa and are considered as two different bilinear approximations for the actual material properties, having linear hardening characteristics in the true stress–true strain domain of 300 MPa and 500 MPa, respectively. Material model *Mat*3, having a yield stress of 105 MPa and a hardening modulus 500 MPa, was selected in order to analyse the influence of the yield stress on the buckling transition.

In all the numerical simulations, the applied initial kinetic energy is 5 kJ, with the gravity force taken into account. This value is approximately the same as the impact energy that causes buckling transition from global bending to a progressive buckling for the tested 500 mm long tubes ($G = 120$ kg, $V_0 = 9$ m/s, $T_0 = 4.86$ kJ, Fig. 4(b)).

4. Features of the buckling transition

The experimental results show that the impact velocity influences significantly the buckling transition due to inertia effects, leading to a significant increase of the critical length. Hence, the tubes tested under quasi-static compression and having a length larger than $L_{cr}^{static} = 315$ mm buckled in a global mode while, for tubes loaded dynamically, the inertia effects, in general, prevent them from a global collapse and the critical length for the buckling transition doubled for impact velocities of around 10 m/s, i.e. $L_{cr}^{dyn} \approx 2L_{cr}^{static}$.

A summary of the numerical simulations is presented in Fig. 6 for the three material models. Similar to the impact tests, tubes of particular lengths between $300 \leqslant L \leqslant 720$ mm were impacted with various masses having initial velocities $2 \leqslant V_0 \leqslant 15$ m/s. The response of each tube length to a low impact velocity was analysed first and if the response was a global collapse, the velocity was slightly increased and the case run again until progressive buckling occurred. The simulations were run as indicated for the three materials. No strain rate effects are taken into account for these material models.

4.1. Buckling shapes at the transition velocities

The numerical study reveals that, as expected, inertia is the major factor governing dynamic buckling transition. However, the material characteristics of a shell also influence the buckling pattern due to the variation in bending rigidity associated with material hardening and yield stress of the material models.

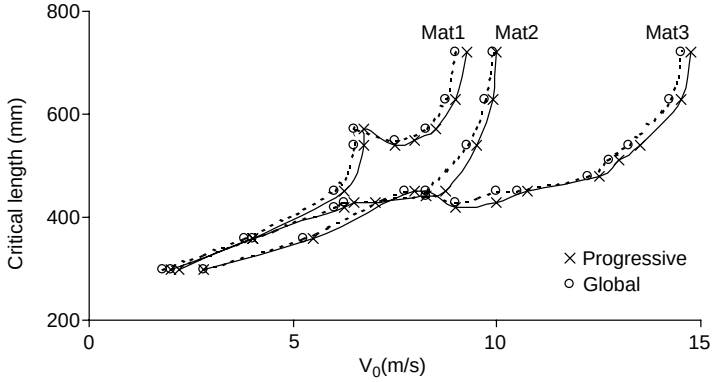

Fig. 6. Influence of the impact velocity on the critical tube length for buckling transition.

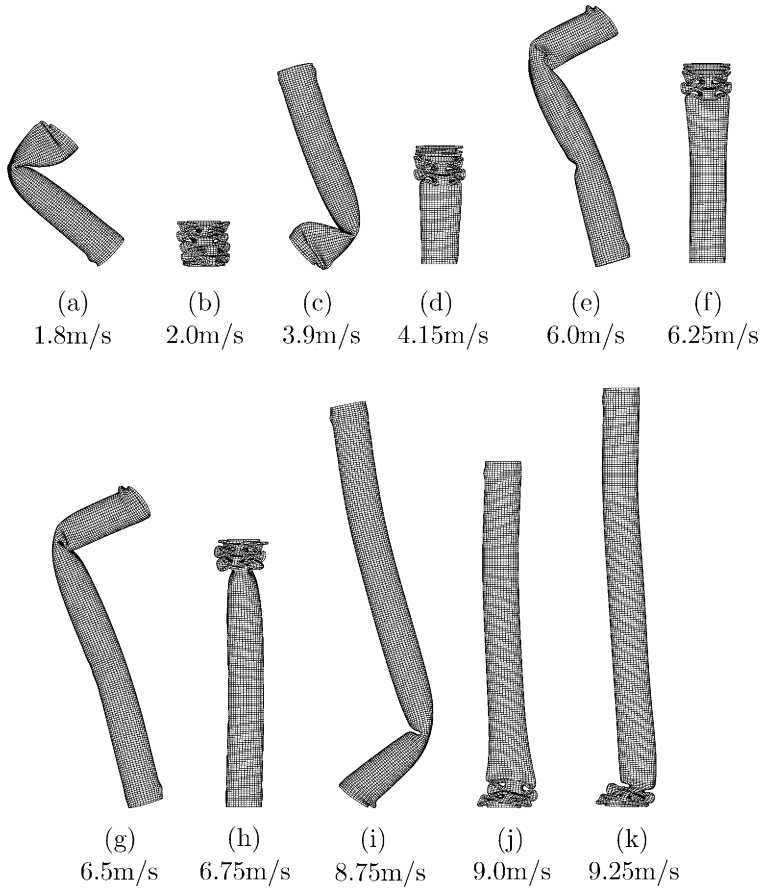

Fig. 7. Collapse shapes at transition impact velocities for tubes made from material *Mat*1. (a,b) $L = 300$ mm, (c,d) $L = 360$ mm, (e,f) $L = 450$ mm, (g,h) $L = 540$ mm, (i,j) $L = 630$ mm, (k) $L = 720$ mm.

The results presented in Fig. 6 show that the tube response stabilises more rapidly for the material having lower strain hardening properties, *Mat*1 (Fig. 7). Accordingly, the lower the hardening modulus the lower the required impact velocity to cause progressive collapse of a tube. A decrease of the hardening modulus affects more significantly the 'shell' response, causing a more rapid growth of the local bending deformations that lead to progressive collapse.

Comparison between the dynamic critical lengths for buckling transition of tubes made from materials *Mat*2 (Fig. 8) and *Mat*3 in Fig. 6 shows that the material yield stress has also a significant effect on the dynamic critical length for transition. This length reduces considerably when decreasing the yield stress while assuming the same strain hardening characteristics. This kind of response is related to the ability of a tube to absorb energy during the initial compressive phase, which depends on the material properties and the impact velocity (Tam and Calladine, 1991). Buckling shapes at selected transition impact velocities are presented in Fig. 9 for material *Mat*3. Obviously, tubes made from this material can absorb less energy during initial compression in comparison to tubes made from material *Mat*2 for the same initial conditions, thus leaving a larger proportion of the initial kinetic energy for the bending phase. Accordingly, a further increase of the impact velocity is required in order to increase the proportion of the energy absorbed in compression and to increase the inertia of the tube.

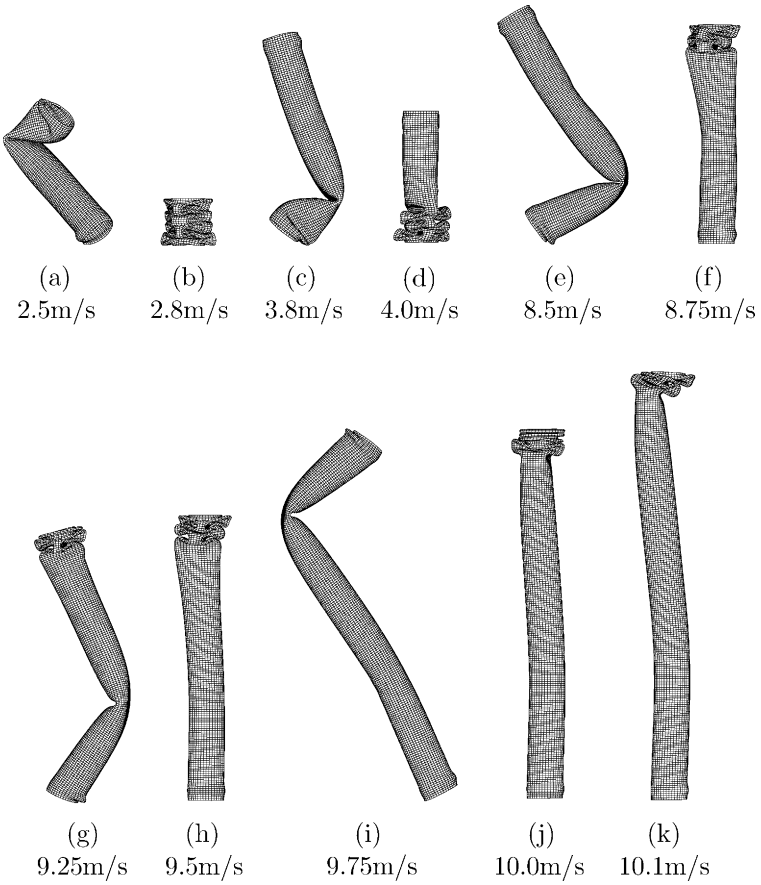

Fig. 8. Collapse shapes at transition impact velocities for tubes made from material *Mat*2. (a,b) $L = 300$ mm, (c,d) $L = 360$ mm, (e,f) $L = 450$ mm, (g,h) $L = 540$ mm, (i,j) $L = 630$ mm, (k) $L = 720$ mm.

4.2. Anomalous dynamic response

The experimental results and the numerical simulations show a general trend of increasing the dynamic critical length when increasing the impact velocity. Nevertheless, an *anomalous* response was revealed by the numerical simulations. Fig. 6 shows that the critical length at the buckling transition can decrease even when the impact velocity increases. This occurs within a small range of impact velocities. Such a response is observed when the location of progressively developed wrinkles changes, e.g. from the proximal to the distal end, as shown in Fig. 10 for material *Mat*1 and $L = 570$ mm.

Global bending occurs for an impact velocity of $V_0 = 6.5$ m/s, as shown in Fig. 10(a) but a slight increase to $V_0 = 6.75$ m/s results in progressive buckling (Fig. 10(b)). However, a further increase of the initial velocity above 6.75 m/s causes a stronger effect on the local bending of the tube by suppressing the rapid growth of the local radial displacements associated with the wrinkle development. The increased local transverse inertia allows for the development of larger global permanent deformations, which results in global bending as evident in Fig. 10(c). A sufficiently large impact velocity increases the global lateral inertia as well as the axial inertia during the early deformation stage. Thus, the tube, which has started to buckle progressively, continues to respond in this buckling mode, Fig. 10(e).

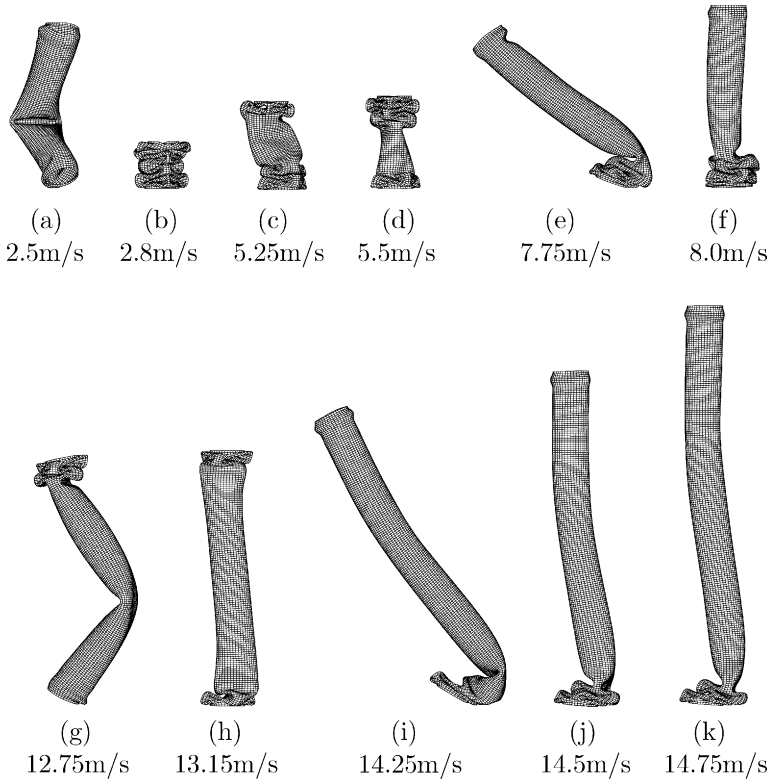

Fig. 9. Collapse shapes at transition impact velocities for tubes made from material *Mat*3. (a,b) $L = 300$ mm, (c,d) $L = 360$ mm, (e,f) $L = 450$ mm, (g,h) $L = 540$ mm, (i,j) $L = 630$ mm, (k) $L = 720$ mm.

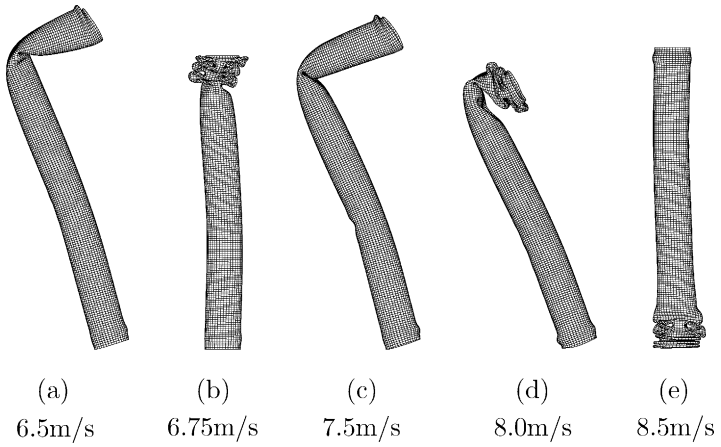

Fig. 10. *Anomalous* response of a tube with $L = 570$ mm made from material *Mat*1.

A similar *anomalous* response is observed in shells made from material *Mat*2 for $L = 420$ mm, but it occurs within a much narrower interval of impact velocities, as shown in Fig. 11. No change of the location

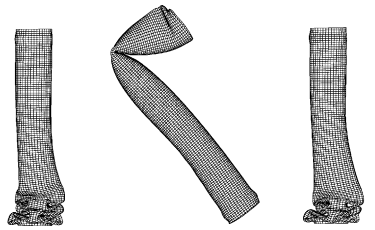

Fig. 11. *Anomalous* response of a tube with $L = 420$ mm made from material *Mat*2.

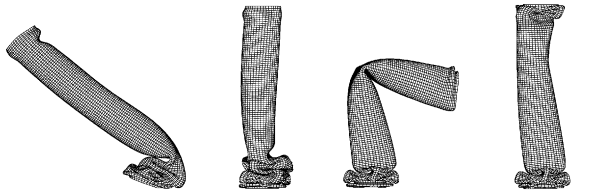

Fig. 12. *Anomalous* response of a tube with $L = 450$ mm made from material *Mat*3.

of the progressively developed wrinkles occurs because of the small variation of the critical tube length for impact velocities between 6.5 and 7.5 m/s.

A more complex response occurs for tubes made from material *Mat*3, for which an *anomalous* response is observed for $L = 450$ mm. In this case, progressive buckling does develop initially near to the distal end of the tube (Fig. 12(b)). However, an increase of the initial velocity above 8 m/s causes a stronger effect on the local bending of a tube by suppressing the rapid growth of the local radial displacements near to the proximal end associated with the wrinkle development. The result is a global bending of the tube in Fig. 12(c). A velocity increase above 10.5 m/s prevents the development of significant permanent global lateral displacements. This allows the development of wrinkles near to the proximal end as well, which stabilises the response, with wrinkles near to both ends, as evident in Fig. 12(d).

4.3. Strain rate effects

Although the aluminium alloy was assumed to be strain-rate insensitive, some simulations were performed for particular tube lengths where small strain rate effect were modelled using the Cowper–Symonds equation with the coefficients $D = 1\,288\,000\ \mathrm{s}^{-1}$ and $q = 4$ (Alves, 2000; Jones, 1974). A significant effect on the critical impact velocity is observed in spite of the very large viscosity constant D.

Strain rate effects cause a global destabilisation of the analysed tubes made from materials *Mat*1 and *Mat*3. Fig. 13(a) shows that a tube with length $L = 630$ mm and made from material *Mat*1 collapses progressively, when assuming a strain-rate insensitive material but responds by a global bending mode to the same impact velocity when strain-rate effects are taken into account, Fig. 13(b). Further increase of the impact velocity is necessary in order to cause progressive buckling collapse for the strain-rate sensitive model, Fig. 13(c). A similar response occurs in a 630 mm long tube made from material *Mat*3 but a much

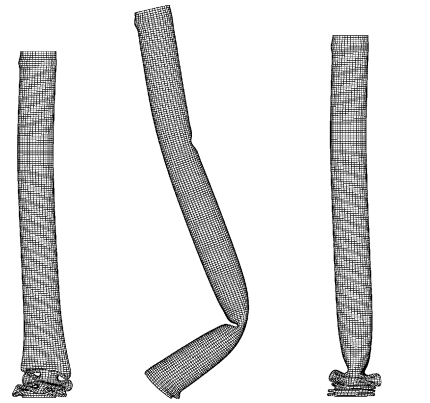

Fig. 13. Buckling transition for a tube with $L = 630$ mm and made from material *Mat*1. (a) No strain rate effect is considered, (b) strain rate effect is taken into account and (c) new transition velocity when strain rate effect is considered.

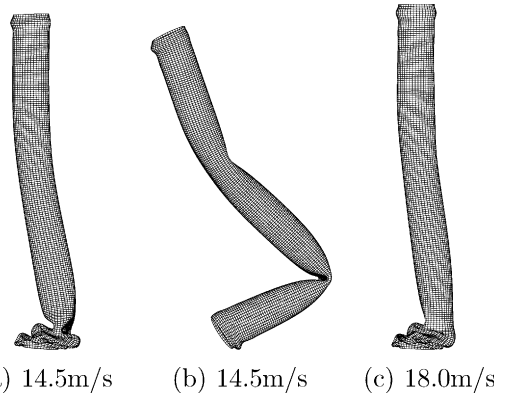

Fig. 14. Buckling transition for a tube with $L = 630$ mm and made from material *Mat*3. (a) No strain rate effect is considered, (b) strain rate effect is taken into account and (c) new transition velocity when strain rate effect is considered.

larger increase of the impact velocity, from 14.5 to 18 m/s, is required in order to obtain dynamic progressive bucking when strain rate effects are taken into account as indicated in Fig. 14.

The assumed material model that considers strain rate effects leads to both a higher material yield stress and larger strain hardening in comparison to a strain rate insensitive material model. Presumably, no significant increase of the absorbed energy during the initial compressive phase occurs, but the increase of the local bending stiffness favours the development of a global buckling mode.

4.4. Energy partitioning

The variation of the critical lengths for the tubes presented in Fig. 6 shows that the material characteristics influence significantly the transition velocities, which increase when increasing the hardening modulus (material *Mat*2) or decreasing the yield stress, as for material *Mat*3. In the case of a constant impact energy, this dependence can be related to the transformation of the initial kinetic energy during the impact event.

Tubes that buckle in the plastic range can absorb energy due to axial compression and through a folding mechanism. It has been established (Karagiozova et al., 2000; Karagiozova and Jones, 2002) that tubes can absorb a considerable proportion of the impact energy during the initial axial compression phase so that less energy remains in the structure for the next phase of folding or bending. Moreover, the initial conditions for the bending phase vary depending on the tube response during the first compressive phase. From this viewpoint, it is important to analyse the energy partition during impact, particularly at the transition conditions, and identify factors causing variation of the energy absorbed during the initial compression phase.

The force-time histories for impacts with initial velocities 8.5 and 8.75 m/s on a 450 mm long shell made from material *Mat*2 are shown in Fig. 15(a). It is evident that the tube responds with an initial axial compression to both impact velocities regardless of the subsequent buckling pattern. During this time, the axial force applied to the proximal end of the tube increases slightly due to material strain hardening. At the end of the compression phase, when $\mathrm{d}F/\mathrm{d}t$ becomes negative, the absorbed energy

$$T_{\mathrm{c}} = \int_{\Omega} \sigma \mathrm{d}\varepsilon_{\mathrm{p}} \approx \int_{0}^{u(t^*)} F(t)\mathrm{d}u(t) \tag{1}$$

is about 600 J (Fig. 15(b)) regardless of the second deformation phase (progressive buckling or global bending). In Eq. (1), Ω is the shell volume and $u(t^*)$ is the axial displacement of the proximal end of the shell at the end of the compression phase at $t = t^*$.

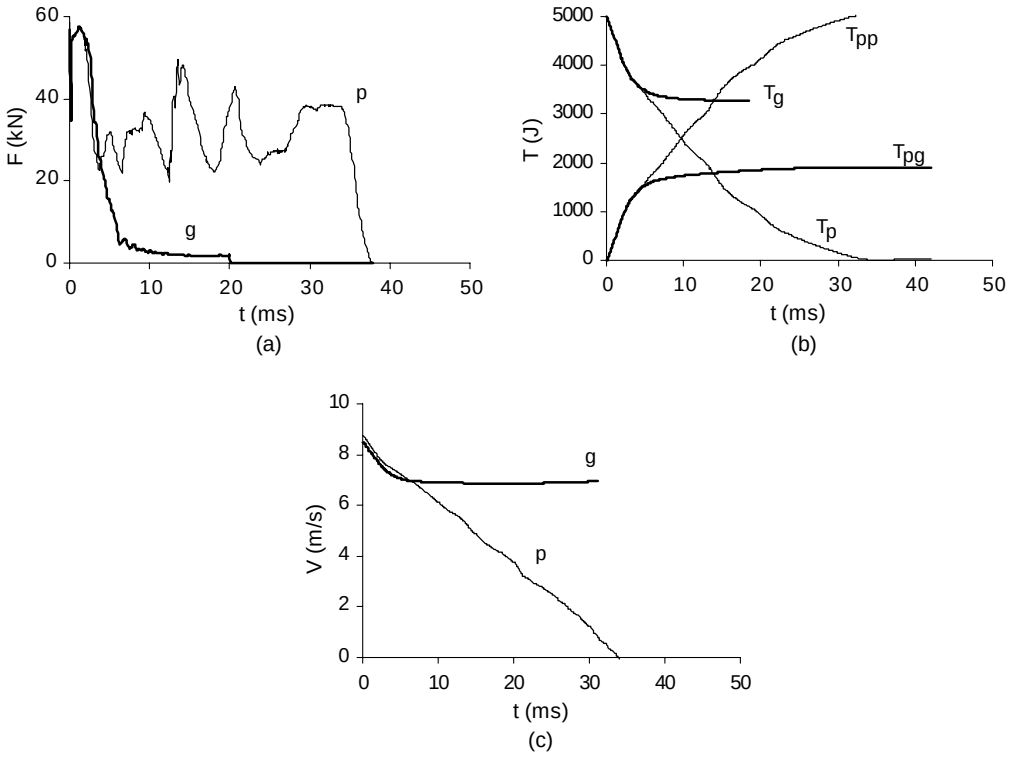

Fig. 15. Response of a shell made from material *Mat*2 having $L = 450$ mm to a 5 kJ axial impact with $V_0 = 8.5$ m/s (g—global collapse) and $V_0 = 8.75$ m/s (p—progressive buckling). (a) Force-time histories, (b) variation of the kinetic (T_k) and plastic dissipation (T_{p}) energy and (c) velocity-time histories.

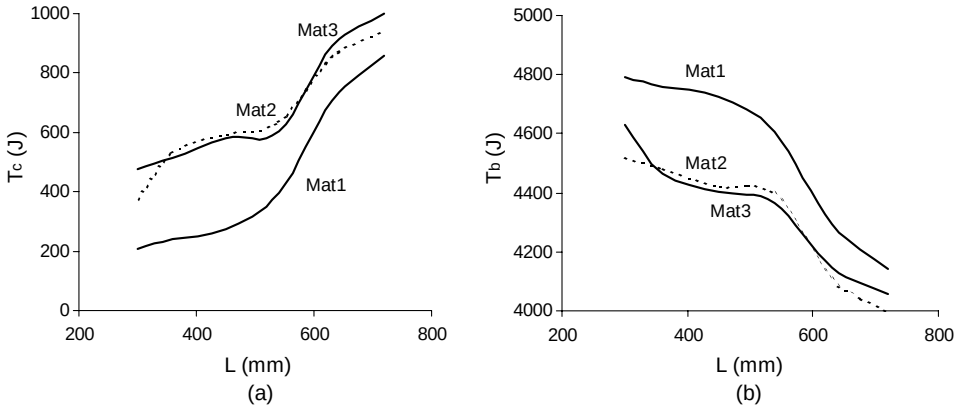

Fig. 16. Energy partitioning in shells at transition velocities shown in Fig. 6 for $T_0 = 5$ kJ. (a) Compression energy and (b) bending energy.

The variation of the compressive energy, T_c, and bending energy, $T_b = T_0 - T_c$, associated with the transition impact velocities for the analysed tubes is shown in Fig. 16 for the three material models used in the numerical simulations. It is evident in Fig. 16(b) that the energy available for global buckling is similar for tubes made from materials with identical hardening characteristics (materials *Mat*2 and *Mat*3) and they can remain stable, i.e. can develop progressive buckling, for similar proportions of the initial kinetic energy. However, higher impact velocities are required to increase the absorbed compressive energy in a tube made from material *Mat*3 as shown in Fig. 6 as this material has a lower yield stress in comparison to material *Mat*2.

On the other hand, tubes made from material *Mat*1 can absorb more energy through the folding mechanism due to the lower strain hardening, leading to a more rapid development of local wrinkles in comparison to material *Mat*2. The above comments are further illustrated when considering an impact by a mass of 138.4 kg having an initial velocity of 8.5 m/s on tubes made from materials *Mat*1 and *Mat*2. In the former case, the tube buckles progressively, Fig. 17(a), while in the later the tube collapses in a global mode, Fig. 17(b). Thus, the dependence of the critical length of a tube on the material properties can also be related not only to the proportion of the initial kinetic energy that a tube can absorb by compression but also to the speed of the development of a local wrinkle, which stabilises the response.

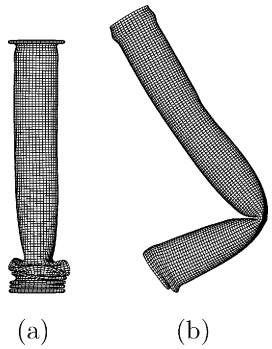

Fig. 17. Influence of the material hardening on the buckling modes for tubes with $L = 450$ mm subjected to an impact with $V_0 = 8.5$ m/s and $G = 138.4$ kg. (a) Material *Mat*1 and (b) Material *Mat*2.

The energy partition during impact shows that the initial compressive phase can cause significant variation of the initial conditions for the subsequent bending phase since they are related to the bending energy as

$$T_b = GV^2(t^*)/2, \tag{2}$$

where $V(t^*)$ is the velocity of the proximal end of a shell at the beginning of the bending phase.

The characteristic features of the dynamic transition from progressive buckling to a global collapse of circular tubes reveal that this complex phenomenon is influenced by the following major factors—loading conditions, inertia of the shell and striker and material properties (yield stress and hardening characteristics).

5. Conclusions

This study establishes the major parameters that govern the dynamic transition between global bending and progressive buckling of circular cylindrical shells subjected to axial impact. The initial experimental findings are further explored by numerical simulations of impacts with various impact velocities on circular tubes made from aluminium alloys with different characteristics.

The experimental study shows that the impact velocity significantly influences the transition conditions between dynamic progressive buckling and a global bending collapse. It was found that not only the inertia effects but also the material characteristics play a significant role in the selection of the buckling mode. Thus, the dynamic buckling transition phenomenon which occurs in circular tubes cannot be analysed assuming a yield stress averaged with respect to the plastic strains when material strain hardening is present. It is evident that the material hardening characteristics have a significant influence on the dynamic collapse mechanisms. Therefore, approximations for the stress–strain relationship as close as possible to the actual stress–strain curve should be considered in theoretical and numerical models for this complex phenomenon, particularly for materials having large strain hardening characteristics.

An *anomalous* response of a shell is observed within small velocity intervals, where the critical buckling length decreases when increasing the impact velocity. This response can be related to a mode interaction and the effects of inertia of the shell and striker.

The present study suggests that circular tubes made from materials with high yield stress and low strain hardening characteristics have better performance as energy absorbers in contrast to tubes made from low yield stress–high strain hardening materials provided that good ductile properties are present in order to avoid material rupture. It should be noted that the conclusions from the present study are based on impact loadings with a constant energy of 5 kJ. Further analysis is required in order to explore the influence of the impact energy on the dynamic buckling transition.

Acknowledgements

The support from the Brazilian funding agency, FAPESP through grants 99/09871-5 and 00/08446-8 and from the Bulgarian National Research Fund, contract TH-1103/01 is greatly acknowledged. The authors are indebted to Prof. N. Jones from the Impact Research Centre, The University of Liverpool, for the valuable discussion on the first draft of this paper.

References

Abramowicz, W., Jones, N., 1997. Transition from initial global bending to progressive buckling of tubes loaded statically and dynamically. International Journal of Impact Engineering 19 (5–6), 415–437.

Alexander, J.M., 1969. An approximate analysis of the collapse of thin cylindrical shells under axial load. Quartely Journal of Mechanics and Applied Mathematics 13, 10–15.

Alghamdi, A.A.A., 2001. Collapsible impact energy absorbers: an overview. Thin-Walled Structures 39, 189–213.

Alves, M., 2000. Material constitutive law for large strains and strain rates. Journal of Engineering Mechanics 126 (2), 215–218.

Alves, M., Karagiozova, D., 2001. Influence of the axial impact velocity on the buckling behaviour of circular cylindrical shells. In: Ivanov, Ya., Baltov, A., Manoach, E. (Eds.), Proceedings of 9th National Congress on Theoretical and Applied Mechanics, Bulgaria. DEMETRA Ltd, Bulgaria, pp. 388–393.

Alves, M., Karagiozova, D., 2002. Dynamic global and progressive buckling of circular shells under impact loads. In: Khan, A.S., Lopez-Pamies, O. (Eds.), Plasticity, Damage and Fracture at Macro, Micro and Nano Scales. Neat Press, Maryland, USA, pp. 621–623.

Andrews, K.R.F., England, G.L., Ghani, E., 1983. Classification of the axial collapse of circular tubes under quasi-static loading. International Journal of Mechanical Sciences 25, 687–696.

Chen, W., Wierzbicki, T., 2001. Relative merits of single cell, multi-cell and foam-filled thin-walled structures in energy absorption. Thin-Walled Structures 39, 287–306.

Guillow, S.R., Lu, G., Grzebieta, R.H., 2001. Quasi-static axial compression of thin-walled circular aluminium tubes. International Journal of Mechanical Sciences 43, 2103–2123.

Hanssen, A.G., Langseth, M., Hopperstad, O.S., 2002. Crash behaviour of foam-based components: validation of numerical simulations. Advances in Engineering Materials 4 (10), 771–776.

Jensen, O., Langseth, M., Hopperstad, O.S., 2002. Transition between progressive and global buckling of aluminium extrusions. In: Jones, N., Brebbia, C.A., Rajandran, A.M. (Eds.), Structures Under Shock and Impact VII. W.I.T. Press, pp. 269–277.

Johnson, W., Reid, S.R., 1978. Metalic energy dissipating systems. In: Steele, C.R. (Ed.), Applied Mechanics Review, vol. 31. pp. 277–288 (see also in Applied Mechanics Update. 1986, pp. 303–319).

Jones, N., 1974. Some remarks on the strain-rate behaviour of shells. In: Sawczuk, A. (Ed.), Problems of Plasticity, vol. 2. Noordhoff, Groningen, pp. 403–407.

Jones, N., 1989a. Recent studies on the dynamic plastic behaviour of structures. Applied Mechanics Review 42, 95–115.

Jones, N., 1989b. Structural Impact. Cambridge University Press, Cambridge.

Karagiozova, D., Jones, N., 1996. Multi–degrees of freedom model for dynamic buckling of an elastic–plastic structure. International Journal of Solids and structures 33 (23), 3377–3398.

Karagiozova, D., Jones, N., 2000. Dynamic elastic–plastic buckling of circular cylindrical shells under axial impact. International Journal of Solids and Structures 37, 2005–2034.

Karagiozova, D., Jones, N., 2001. Influence of stress waves on the dynamic progressive and dynamic plastic buckling of cylindrical shells. International Journal of Solids and Structures 38, 6723–6749.

Karagiozova, D., Jones, N., 2002. On dynamic buckling phenomena in axially loaded elastic–plastic cylindrical shells. International Journal of Non-Linear Mechanics 37, 1223–1238.

Karagiozova, D., Alves, M., 2004. Transition from progressive buckling to global bending of circular shells under axial impact—Part II: Theoretical analysis. International Journal of Solids and Structures, in this issue.

Karagiozova, D., Alves, M., Jones, N., 2000. Inertia effects in axisymmetrically deformed cylindrical shells under axial impact. International Journal of Impact Engineering 24 (10), 1083–1115.

Lu, F., Mao, R., 2001. A study of the plastic buckling of axially compressed cylindrical shells with a thick-shell theory. International Journal of Mechanical Sciences 43, 2319–2330.

Mahmood, H.F., Paluszny, A., 1982. Stability of plate-type box columns under crush loading. In: Computational Methods in Ground Transportation Vehicles, AMD-Vol. 50. Winter Annual Meeting of ASME, pp. 17–33.

Mazzolani, F.M., 1985. Aluminium alloy structures. Rittman Advanced Publishing Program, Boston (Mass).

Reid, S.R., 1993. Plastic deformation mechanisms in axially compressed metal tube used as impact energy absorbers. International Journal of Mechanical Sciences 35 (12), 1035–1052.

Reid, S.R., Reddy, T.Y., Peng, C., 1993. Dynamic compression of cellular structures and materials. In: Jones, N., Wierzbicki, T. (Eds.), Structural Crashworthiness and Failure. Elsevier Science Publishers, Barking, Essex, pp. 295–340.

Su, X.Y., Yu, T.X., Reid, S.R., 1995. Inertia sensitive impact energy absorbing systems. Part I—Effect of inertia and elasticity. International Journal of Impact Engineering 16, 561–672.

Tam, L.L., Calladine, C.R., 1991. Inertia and strain-rate effects in a simple plate-structure under impact loading. International Journal of Impact Engineering 11, 349–377.